

KINETICS OF DEFORMATION AND DAMAGE ACCUMULATION
IN CONCENTRATION ZONES WITH NONISOTHERMAL
LOW-CYCLE LOADING

A. G. Kazantsev, A. P. Gusenkov,
and A. N. Chernykh

UDC 539.4

With currently existing strength safety factors, in the majority of structures, only concentration zones in the material operate beyond the elastic limit, and the main part of the metal structure deforms elastically. In view of this, the supporting capacity of structural elements is governed primarily by the stress-strain state and strength conditions in areas of concentration. Since generally the properties of a material may vary in relation to the number of loading cycles, the process of deformation and damage accumulation in local zones of a structure is characterized by certain transience.

The change in stress-strain state (SSS) and the nature of damage accumulation in concentration zones, according to the number of loading cycles, has been studied most at normal and high constant temperatures [1-3]. In the case of nonisothermal loading, a series of additional features arise. With a constant nominal stress amplitude, the amount of maximum cyclic deformation in concentration zones depends not only on the range of change in temperature, but also on the phase of superimposition of the temperature cycle on the force-loading cycle. The amount of damage accumulation in the general case is governed by parameters of the temperature cycle, by the dependence of the available plasticity for the test material on temperature and time, and by the form of the stress state and other factors [4, 5].

As the simplest temperature-force schedules it is desirable to isolate those with linear synphase and counterphase variation of load and temperature in the cycle (Fig. 1). These schedules are comparatively easily realized in experiments, and during calculation of the stress-strain state it is possible to use the simplest approach of ideas about the surface of thermomechanical cyclic loading [6-9].

Data are given in the present work for endurance with nonisothermal loading of steel 15Kh2MFA specimens with elastic stress-concentration factors $\alpha_\sigma = 2.5$ and 3.5. Results and test procedure with $T = \text{const}$ are given in detail in [8]. In the gage length specimens are a plate 1.5 mm thick and 40 mm wide having sharp side notches ($\alpha_\sigma = 3.5$) and a round central hole ($\alpha_\sigma = 2.5$) (see Fig. 2).

Specimen heating was carried out in a low-inertia furnace with a quartz-halogen lamp of the KGM type [10]. In order to increase the rate of heat removal from the specimen, water cooling was installed on the grips. In the case of nonisothermal tests temperature was varied in the range 100-500°C, and with isothermal loading $T_{\text{max}} = 500^\circ\text{C} = \text{const}$, which corresponds to the operating temperature level for the test steel. Duration of the heating-cooling cycle was about 4 min.

On the basis of experimental measurements it was established that the heating method used provides quite a uniform field around the concentrator in the specimen plane. The temperature drop through the thickness did not exceed 8-10°C with $T_{\text{max}} = 500^\circ\text{C}$. It is typical that temperature distribution with the heating-cooling rates adopted differs insignificantly from that with steady heating in the case of $T = \text{const}$.

Use was made in the tests of modernized programmed equipment type UM-10, making it possible to synchronize, by means of a program selector type RU-5-01 with an additional slide wire, in the required phase loading and heating cycles. Specimen loading was accomplished by a cycle from zero. The instant of failure was recorded by means of a microscope from formation of a visible crack. During tests one-sided accumulated and cyclic deformation was

Institute of Mechanical Engineering, Academy of Sciences of the USSR, Moscow. Translated from *Problemy Prochnosti*, No. 8, pp. 19-24, August, 1985. Original article submitted June 14, 1984.

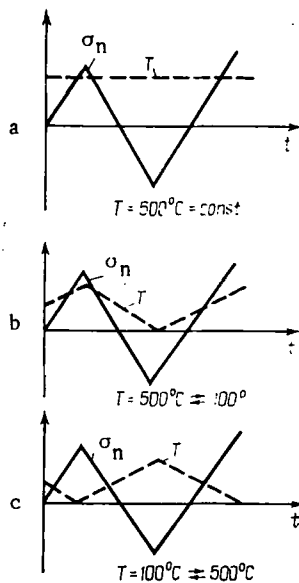


Fig. 1. Loading schedules.

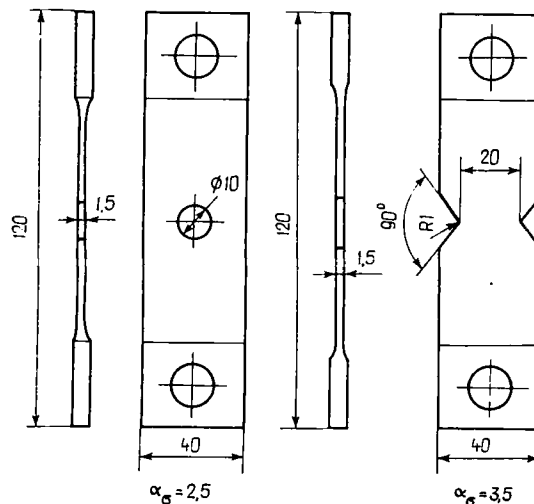


Fig. 2. Test specimens.

measured in concentration zones. With this in mind the specimen surface was chromized and a square network with a pitch of 0.25 mm was applied. Deformation in two directions in the specimen plane was measured by a microscope with a magnification of $\times 130$. The third component was determined from the condition for noncompressibility.

In order to isolate the thermal component of deformation, prior thermal cycling was carried out without a load.

In the load range studied different types of failure were obtained for specimens with concentrations: fatigue, mixed, and quasistatic. The nature of failure was governed by the level of nominal stresses, the degree of concentration, and also by the test combination of load and heating cycles.

As the results of tests show, the number of cycles to failure depends to a marked degree on the phase of superimposition of the temperature cycle on the loading cycle. The value of endurance with synphase loading appears close to data for $T = 500^\circ\text{C} = \text{const}$. With counterphase loading the number of cycles to failure was on average two to five times greater than with synphase loading and $T = 500^\circ\text{C} = \text{const}$ (Fig. 3). It was typical that with tension-compression tests for smooth specimens (without concentration zones) under synphase and counterphase loading conditions with a similar cycle duration this effect was absent [5]. In this case, results of all tests lie almost on one curve (Fig. 4).

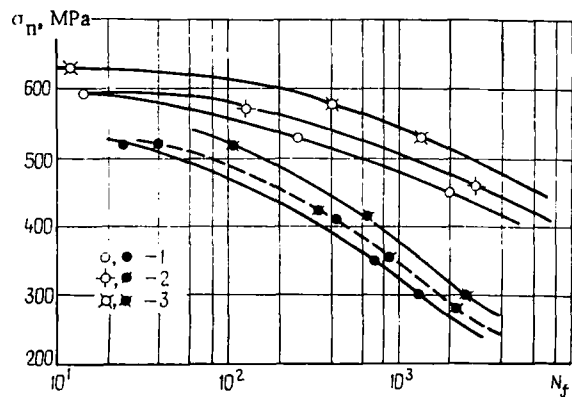


Fig. 3. Low-cycle fatigue curves for specimens with $\alpha_\sigma = 2.5$ (open points) and $\alpha_\sigma = 3.5$ (shaded points) with soft loading: 1) $T = 500^\circ\text{C} = \text{const}$; 2) $T = 100^\circ\text{C} \rightleftharpoons 500^\circ\text{C}$; 3) $T = 500^\circ\text{C} \rightleftharpoons 100^\circ\text{C}$ (σ_n is the nominal stress range in the net cross section; N_f is the number of cycles to crack formation).

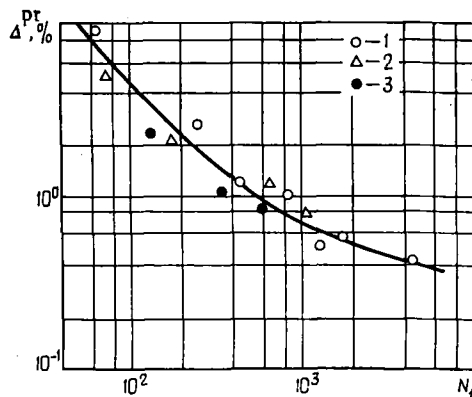


Fig. 4. Low-cycle fatigue curves for smooth specimens of steel 15Kh2MFA with hard loading: 1) $T = 500^\circ\text{C} = \text{const}$; 2) $T = 500^\circ\text{C} \rightleftharpoons 100^\circ\text{C}$; 3) $T = 100^\circ\text{C} \rightleftharpoons 500^\circ\text{C}$ (ΔP^E is elasto-plastic deformation range).

The nature of change in the endurance of specimens with concentration zones agrees with measured data for maximum deformation carried out by the network method (Fig. 5). As follows from Fig. 5, for a synphase schedule and $T = 500^\circ\text{C} = \text{const}$ the range of deformation appeared quite close, and with counterphase loading its value was less than in the first two cases. The range of deformation in relation to the number of loading cycles increases a little, which is caused by cyclic loss of strength for the material. Similar dependences are observed for one-sided accumulated deformation. The process of one-sided deformation accumulation is most strongly expressed with high nominal stress levels. In the range of endurances $N_f > 5000 \dots 10000$ the deformation schedule at the edge of concentrators is close to hard, with insignificant accumulation of one-sided deformation.

Apart from the network method, in order to determine the SSS in concentration zones and to study its kinetics in view of the cyclic properties of the material, numerical calculations were carried out by the finite element method. In order to describe the cyclic properties of the material with $T = \text{const}$, use was made of ideas about the generalized cyclic deformation diagram. Deformation curves with nonisothermal loading were described on the basis of an approach [7] suggesting existence of a cyclic thermomechanical loading surface on coordinates $\sigma - \epsilon - T$.

In view of the considerable complexity and difficulty of studying all of the deformation kinetics with an increase in the number of cycles, calculation was carried out assuming a hard loading schedule in concentration zones with unregulated strain amplitude as a result

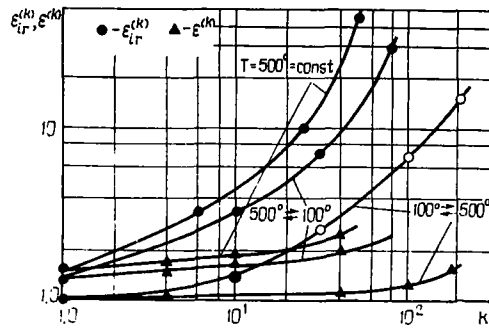


Fig. 5. Dependence of the intensity of one-sided accumulated and cyclic deformation on number of loading half-cycles ($\sigma_n = 520$ MPa; $\alpha_\sigma = 3.5$).

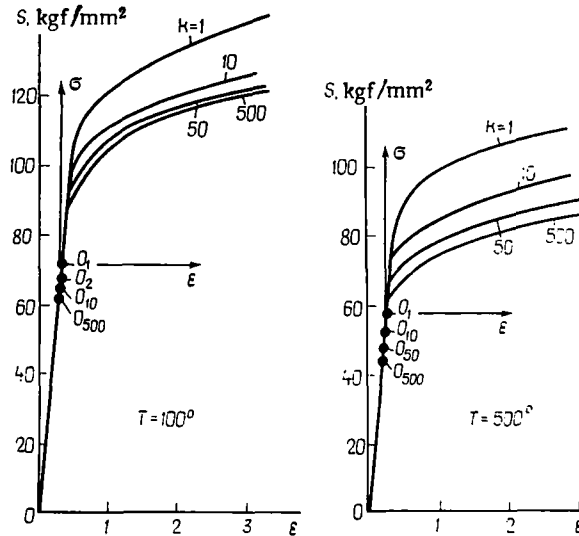


Fig. 6. Cyclic deformation curves for steel 15Kh2MFA on coordinates $S-\epsilon$ (combined with the point for the start of loading) and $\sigma-\epsilon$ ($O_1, O_{10}, O_{50}, O_{500}$ are the positions for the start of coordinates of $\sigma-\epsilon$ in half cycles $k = 1, 10$, etc.).

of material cyclic loss of strength. This approach does not make it possible to analyze the upper part of the fatigue curves (Fig. 3), since in this case it is necessary to have a more accurate description of material properties and to use an improved calculation procedure. However, it embraces the more important cases of failure from a practical point of view, close to fatigue failure when one-sided deformation accumulation may be ignored.

With calculation in each of the half-cycles use was made of a single loading region over the whole deformation curve on coordinates $S-\epsilon$ (Fig. 6). With $T = \text{const}$ this curve is similar to the generalized cyclic deformation curve. With the aim of determining the SSS in the case of nonisothermal deformation, in accordance with ideas about the existence of a thermomechanical loading surface, calculation was carried out for finite values of temperature in half cycles. In the zero half-cycle with sections of this surface at $T = \text{const}$ there are normal static deformation curves. Use was made of the amount of plastic deformation in the $k-1$ half-cycle as a parameter with cyclic loading governing the position of thermomechanical surface on coordinates $\sigma-\epsilon-T$ in the k -th half-cycle.

As shown in [7], the current point of the cyclic nonisothermal deformation curve lies on surface $\sigma-\epsilon-T$ plotted from the results of isothermal tests with the condition that under isothermal loading in each of the preceding half-cycles the amount of plastic deformation agrees with the corresponding value obtained for the nonisothermal schedule.

TABLE 1. Calculated and Experimental Values of Endurance and Cyclic Deformation for Isothermal and Nonisothermal Loading Schedules

σ_n , MPa	α_σ	$T=500^\circ\text{C}=\text{const}$				$T=500^\circ\text{C}\rightarrow 100^\circ\text{C}$				$T=100^\circ\text{C}\leftarrow 500^\circ\text{C}$			
		ϵ_t	ϵ_{pl}	N_{calc}	N_{exp}	ϵ_t	ϵ_{pl}	N_{calc}	N_{exp}	ϵ_t	ϵ_{pl}	N_{calc}	N_{exp}
460	3,5	0,823	0,43	760	1400	0,671	0,32	1200	2500	0,515	0,157	2000	5000
500	2,5	0,919	0,526	620	550	0,873	0,477	680	1100	0,546	0,177	1500	2400
590	2,5	1,34	0,93	400	15	1,18	0,752	430	70	0,82	0,44	750	300
300	3,5	0,818	0,424	780	1400	0,66	0,30	1200	1700	0,486	0,137	2500	2500
420	3,5	1,26	0,85	420	350	1,01	0,703	550	350	0,762	0,366	880	650
500	3,5	2,70	2,24	160	60	1,8	1,44	250	70	1,22	0,795	430	150

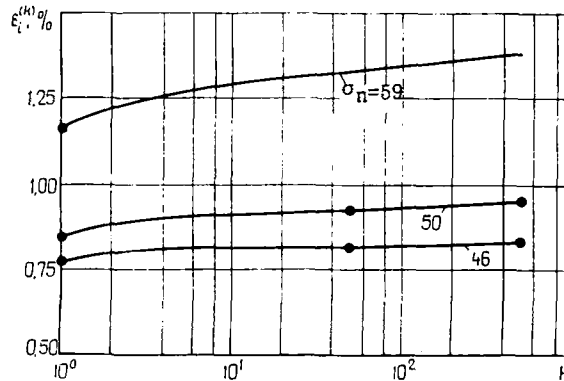


Fig. 7. Change in maximum calculated deformation in relation to the number of loading half-cycles with $T = 500^\circ\text{C} = \text{const}$.

In accordance with the approach adopted, a schedule with a linear change in temperature in the cycle may be substituted by an equivalent schedule with a gradual transition from T_{max} to T_{min} (or conversely) in extreme points of the cycle. Solution of the problem was accomplished for the fixed temperature values indicated. In plotting $S-\epsilon$ curves sections of elastic unloading were added to $\sigma-\epsilon$ diagrams (Fig. 6) determined from the results of solving the problem in the preceding half-cycle, and in this way the dependence of residual stresses on elasticity modulus was considered.

Calculation with the prescribed loading cycle starting from zero indicates that in concentration zones the deformation schedule is characterized by certain kinetics for cyclic deformation. In the zero half-cycle (initial loading), for all of the cases considered, deformation has the maximum value. In the first and subsequent half-cycles it is less than in the zero half-cycle, and with an increase in the number of half-cycles the amount of deformation increases a little, which is caused by material cyclic loss of strength.

As an example Fig. 7 shows the change in maximum values of deformation intensity $\epsilon_i \max$ at the edge of the hole for $\alpha_\sigma = 2.5$ with $\sigma_n = 460, 500, \text{ and } 590$ MPa. The rate of failure with increasing number of loading half-cycles slows down, particularly for lower values of nominal stresses, which are governed by the nature of change in the cyclic deformation diagram (Fig. 6).

Comparison of the calculated deformation values for isothermal and nonisothermal synphase and counterphase loading schedules (Table 1) indicates that with the same level of nominal stresses under isothermal loading with $T = T_{max} = 500^\circ\text{C}$ the range of deformation appears to be markedly higher than with counterphase loading, and close to the corresponding value for synphase schedules, as was obtained with measurements by the network method (Fig. 5).

The greatest difference is observed for plastic deformation. Values given in Table 1 relate to the half-cycle $k = 100$. The nature of change in deformation in relation to the number of half-cycles with nonisothermal loading is similar to that shown in Fig. 7 for $T = 500^\circ\text{C} = \text{const}$.

For calculated determination of the endurance of specimens with concentration zones, use was made of the deformation approach [4] and a rule for linear summation of fatigue damage in the form

TABLE 2. Calculated Values for Isothermal and Nonisothermal Loading Schedules

σ_n , MPa	N_{exp}	ϵ_{ir} , %	d_f	d_s	d_Σ	N_{calc}	α_σ	Schedule, °C
440	2000	7,57	2,0	0,097	2,1	950	2,5	500
520	240	24,4	0,413	0,32	0,733	328	2,5	500
590	15	47,8	0,04	0,615	0,619	24	2,5	500
300	1400	2,9	1,8	0,04	1,84	761	3,5	500
350	750	4,0	1,25	0,055	1,3	577	3,5	500
420	420	6,3	0,715	0,086	0,8	375	3,5	500
518	25	37,2	0,16	0,617	0,78	36	3,5	500
455	2800	5,46	2,08	0,06	2,15	1300	2,5	500↔100
570	140	81,8	0,28	1,05	1,33	338	2,5	500↔100
280	2300	5,85	0,583	0,08	0,66	3500	3,5	500↔100
360	900	7,8	1,13	0,1	1,23	732	3,5	500↔100
420	350	30,0	0,636	0,41	1,05	334	3,5	500↔100
510	40	54	0,2	0,74	0,94	43	3,5	500↔100
540	1500	4,68	1,5	0,06	1,56	960	2,5	100↔500
580	400	15,6	0,64	0,22	0,84	535	2,5	100↔500
630	12	93,5	0,02	1,2	1,22	10	2,5	100↔500
300	2500	5,1	1,0	0,07	1,07	2340	3,5	100↔500
420	550	11,0	0,625	0,15	0,775	710	3,5	100↔500
510	105	23,4	0,3	0,32	0,62	170	3,5	100↔500

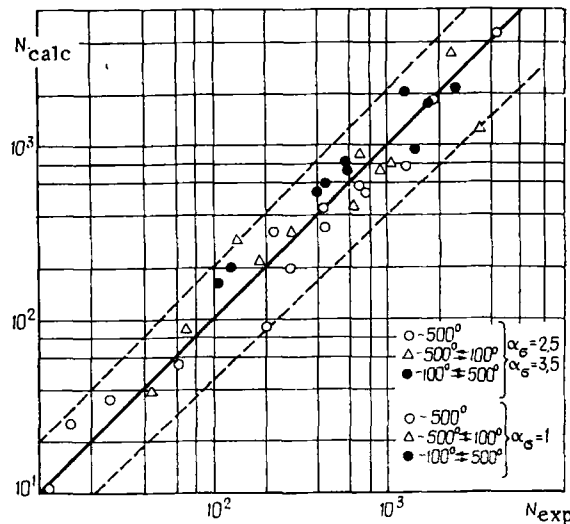


Fig. 8. Comparison of calculated and experimental values of endurance.

$$d_f = \sum \frac{n}{N_i} = 1, \quad (1)$$

where n is number of loading cycles for the schedule considered with a range of deformation corresponding on the fatigue curve (Fig. 4) to endurance N_i .

As a result of the fact that original fatigue curves for smooth specimens with $T = 500^\circ\text{C} = \text{const}$ and for nonisothermal schedules $100 \nleftrightarrow 500^\circ\text{C}$ and $500 \nleftrightarrow 100^\circ\text{C}$ almost coincide (Fig. 4), in those cases when the ranges of deformation in the concentration zones with $\sigma_n = \text{const}$ differ, calculated values for endurance also appear to be different, which agrees with the results of experiments (Fig. 3).

As follows from Table 1, calculated values of endurance are in good agreement with experimental data N_{exp} with nominal stresses $\sigma_n = 460$ and 500 MPa for $\alpha_\sigma = 2.5$, and $\sigma_n = 300$ and 400 MPa for $\alpha_\sigma = 3.5$. Discrepancies obtained with higher values of σ_n (in particular for $T = 500^\circ\text{C} = \text{const}$) are caused by the fact that no consideration is given in the calculation to accumulation of one-sided deformation, which is most marked for high nominal stress levels.

For example, it may be assessed from the results of measurements by the network method, and the endurance value may be determined from the condition

$$d_f + d_s = 1, \quad (2)$$

where $d_n = \frac{\epsilon_f}{\epsilon_f}$ is quasistatic damage; ϵ_{fR} is intensity of one-sided deformation accumulation; ϵ_f is limiting deformation with static tension, which for steel 15Kh2MFA is a stable characteristic independent of loading duration and form of heating cycle [5]. Taking account of the volumetric nature of the stress state in concentration zones, its value is 73-78% [2].

In using (2), conformity of calculated and experimental results, as follows from Fig. 8 and Table 2, appears to be satisfactory for all of the test stress levels. Also shown in Fig. 8 is the scatter limit of endurance values for smooth specimens from results presented in Fig. 4.

In all of the cases of loading for specimens with concentration zones, the discrepancy in calculated (taking account of quasistatic damage) and experimental values of endurance does not exceed the scatter limits of the corresponding values of smooth specimens.

In conclusion, it is noted that the difference in endurance values for the test material in concentration zones with isothermal and nonisothermal loading schedules is only caused by deformation properties of the material in the temperature range considered. For a number of materials, as noted above, synphase and counterphase loading schedules, and also isothermal loading with $T = T_{\max} = \text{const}$, are characterized in addition by different damage, and consequently the relative position of the fatigue curves for concentration zones with nonisothermal loading schedules and $T_{\max} = \text{const}$ may differ from those obtained in the case given, as shown in [11] in studying steel Kh18N9.

LITERATURE CITED

1. A. P. Gusenkov, Strength with Isothermal and Nonisothermal Low-Cycle Loading [in Russian], Nauka, Moscow (1979).
2. N. A. Makhutov, Deformation Criteria and Engineering Design of Structural Elements [in Russian], Mashinostroenie, Moscow (1981).
3. N. A. Makhutov and A. N. Romanov (eds.), Strength of Structures Under Low-Cycle Loading [in Russian], Nauka, Moscow (1983).
4. A. G. Kazantsev, "Resistance of materials to low-cycle fatigue with nonisothermal loading," Probl. Prochn., No. 7, 3-8 (1983).
5. A. G. Kazantsev, A. N. Chernykh, and A. P. Gusenkov, "Study of failure mechanisms with low-cycle nonisothermal loading," Zavod. Lab., 49, No. 1, 74-78 (1983).
6. I. A. Birger, B. S. Shorr, I. V. Dem'yanushko, et al., Thermal Strength of Machine Components [in Russian], Mashinostroenie, Moscow (1975).
7. A. P. Gusenkov and A. G. Kazantsev, "Equations of state with nonisothermal loading," in: Equations of State with Low-Cycle Loading [in Russian], Nauka, Moscow (1981).
8. V. V. Moskvitin, Cyclic Loading of Structural Elements [in Russian], Nauka, Moscow (1981).
9. Yu. N. Shevchenko, "Approximation methods for solving the problem of thermoplasticity taking account of loading history," Teplovye Napryazheniya v Élementakh Konstruktsii, No. 7, 37-48 (1967).
10. A. M. Zakharov, "Development of automatic mechanical tests," in: Resistance of Materials to Corrosive Agents [in Russian], Krasnodar Inst. (1977).
11. A. P. Gusenkov and A. G. Kazantsev, "Strength with low-cycle and prolonged cyclic deformation in view of the shape of loading and heating cycles," Mashinovedenie, No. 3, 59-65 (1979).